Regional Studies in Marine Science
December 2023, Volume 65, Pages 103110 (12p.)
https://doi.org/10.1016/j.rsma.2023.103110 https://archimer.ifremer.fr/doc/00847/95881/

First Characterization of *Protoceratium reticulatum* (Dinophyceae) from Atlantic coast of Morocco: Growth experiment, molecular identification, and toxicity

Moussavou-Mouity Cyrielle Amour [1, *], Ababou Bouchra [1], Herve Fabienne [2], Tanniou Simon [2], Amzil Zouher [2], Bennouna Asmae [3]

[1] Hassan First University, PO box 539, 26000, Settat, Morocco
[2] IFREMER, PHYTOX Unit, METALG Laboratory, F-44300 Nantes, France
[3] National Institute of Fisheries Research (INRH), LSSMM regional center, PO box 80000, Agadir, Morocco

* Corresponding author : Cyrielle Amour Moussavou-Mouity, email address : c.moussavou-mouity@uhp.ac.ma

Abstract :

Protoceratium reticulatum is a dinoflagellate recognized as a producer of yessotoxin and its analogues. It grows over a wide range of temperature, irradiance, nutrients, salinity, and pH. There is limited research on toxic dinoflagellates in Moroccan coastal areas. Therefore, for the first time, P. reticulatum was isolated from the Agadir coast in the Imiouaddar shellfish growing area (Morocco, Atlantic), and monoclonal cultures were established. For growth experiments, cultures were exposed to three temperatures (15, 20, and 25 °C), three levels of irradiance (20, 80, and 130 µmol. m−2. s−1), and five concentrations of nitrate/phosphate concentrations of L1 culture medium (L1, 1.5 L1, 2 L1, 2.5 L1, 3 L1). Molecular analysis of the 18S rDNA gene confirmed the identity of our P. reticulatum strain. The strain was grown only at 20 °C. Temperatures of 15 and 25 °C induced cell death. Different levels of irradiance and nutrients did not influence its maximum growth rate. However, the 3 L1 culture medium significantly impacted maximum cell density. Despite the combination of all the more or less optimal parameters (20 °C, 80 µmol. m−2. s−1, L1 medium), the maximum growth rate remained low: 0.29 div. day −1. The cell lysate of P. reticulatum significantly affected the survival of Artemia salina nauplii. The analysis of toxins by liquid chromatography with tandem mass spectrometry (LC-MS/ MS) of P. reticulatum culture extract revealed that the species was able to produce yessotoxin at a concentration of 27.0 ± 2.60 pg YTX cell −1. Until now, no bloom of P. reticulatum has been reported on the Atlantic coast of Agadir. However, in Moroccan coastal waters, an “early warning” system has already been established to better control shellfish growing areas in the event of a bloom of this species.

Graphical abstract

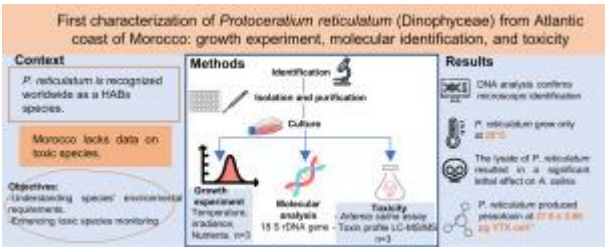

Highlights

► First isolation and culture of the dinoflagellate *P. reticulatum* in Morocco. ► First molecular identification of a *P. reticulatum* strain in Morocco. ► First report about YTX production by *P. reticulatum* isolated in the Atlantic of Morocco.

Keywords : Dinoflagellates, Yessotoxins, LC-MS/MS, Artemia salina, Growth rate

1. Introduction

Protoceratium reticulatum (Claparède and Lachmann) Bütschli 1885, is a photosynthetic and thecate planktonic dinoflagellate that belongs to the family Gonyaulacaceae (Hansen et al., 1997). It is a fairly common and widely distributed species in coastal waters worldwide. According to Rodríguez et al. (2007), it is reasonable to assume that *P. reticulatum* can grow in a wide range of temperature, salinity, light, pH, and nutrient conditions. In cultures, *P. reticulatum* was first identified as a yessotoxin (YTX) producer in New Zealand by Satake et al. (1998). Subsequently, YTX has been found in *P. reticulatum* from different locations; Japan (Satake et al., 1999; Eiki et al., 2005; Suzuki et al., 2007), the Adriatic Sea in Italy (Ciminiello et al., 2003), Nova Scotia, Canada (Stobo et al., 2003), Norway (Samdal et al., 2004), Spain (Paz et al., 2004; Paz et al., 2007) and Argentina (Akselman et al., 2015).

Yessotoxins (YTXs) are a group of structurally disulphated polyether toxins, which were first isolated by Murata et al. (1987) from the scallop *Patinopecten yessoensis* after a red tide in Japan. YTX is mainly produced by the marine dinoflagellates *P. reticulatum, Lingulodinium polyedra* (Draisci et al., 1999), and *Gonyaulax spinifera* (Rhodes et al., 2004). However, *P. reticulatum* is the most studied since it is the origin of the majority of toxins in the YTX group among dinoflagellate producers (Miles et al., 2005). The YTX group has over 100 analogues reported in bivalves or dinoflagellates. Despite this large variability in the reported toxin profile, it appears that the main toxin of *P. reticulatum* is generally YTX (Paz et al., 2007). However, the toxin profile in different *P. reticulatum* strains has been found to depend on the origin of the strain (Eiki et al., 2005; Paz et al., 2007).

YTX production has been shown to occur during all phases of growth in batch culture of *P. reticulatum* strains, and toxins are contained in the cells and the culture medium (Paz et al., 2013). They are also highly toxic to mice by intraperitoneal injection rather than oral administration (Aune et al., 2002). There are reports of damage to the heart muscle (Aune et al., 2002), liver and pancreas (Terao et al., 1990), and neural tissue (Franchini et al., 2004) by intraperitoneal administration of YTX supply in mice.

Yessotoxin group toxins (YTXs) have been detected worldwide in filter-feeding bivalve mollusks (e.g., mussels, oysters, scallops). They may present a health risk to the consumer. As there are no reports of adverse effects in humans associated with YTX, the European Commission increased the health threshold in 2013 from 1 to 3.75 mg YTX equivalent kg^{-1} shellfish meat (European Community, 2013).

In this study, we report the first cultures of *P. reticulatum* strain from the Atlantic coasts of Morocco, as well as the confirmation of yessotoxins (YTXs) production, their characterization, and quantification. A phylogenetic analysis of the 18S small subunit (SSU) ribosomal gene was performed to confirm strain identity and to assess the genetic relationships between our Moroccan strain and others existing in the GenBank (The National Center for Biotechnology Information). We determined the optimal conditions for the growth of our *P. reticulatum* strain in terms of temperature, light, and nutrients. We also evaluated the effect of intracellular toxins of *P. reticulatum* on the survival of brine shrimp *Artemia salina*.

2. Materials and Methods

2.1. Isolation and establishment of the culture

Protoceratium reticulatum was collected using a phytoplankton net (20 µm) from the Imiouaddar shellfish growing area (Agadir) in the Atlantic of Morocco (30°35'26.8''N 9°48'04.0''W) in July and August 2021, with sea surface temperatures ranging from 18 to 20 °C.

Cultures were initially established by picking single cells using a capillary pipette (Tsuchikane et al., 2018) and incubating them in silica-free L1 medium (Guillard and Hargraves, 1993) at a salinity of 36 in microplates (96 well). All cultures of the *P. reticulatum* strain (provisionally named IMD1) were monoclonal. Cells were examined daily under an inverted microscope (Leica Microsystems DMi8) to ensure the purity of the strains. Cultures were transferred in 100 mL Erlenmeyer flasks containing L1 medium under a 12:12 h light: dark cycle, an irradiance of 80 µmol. m^{-2}. s^{-1} and at a temperature of 20 °C.

2.2. Cell morphology

Morphology was determined using an inverted microscope (Leica microsystems, DMi8) and a right fluorescence microscope (Leica, DM 1000). Cells in exponential phases were fixed with Lugol's acid solution and counted at 400 X magnification. The length and width of 30 cells were measured using the progressive microscope cameras software analysis tool, JENOPTIK.

Identification was based on visual observation of the general characters and remarkable morphological attributes of the cells, that is, according to shape, size, and presence of theca (Lassus et al., 2016).

2.3. Molecular phylogenic analysis

The Roscoff Culture Collection laboratory performed molecular analysis of the 18S rDNA small subunit (SSU) gene. A BLAST search was performed with the 18S rDNA sequence obtained, and the resulting 18S SSU sequences of other *P. reticulatum* strains were extracted from the GenBank (NCBI database http://www.ncbi.nlm.nih.gov/).

Sequences of *P. reticulatum* and other sequences were aligned. The additional sequences of *P. reticulatum* corresponded to those that showed a relationship with our IMD1 strain in BLAST. A sequence of *Prorocentrum micans* was included as an outgroup. The resulting alignment was restricted to the sequence strain length of the IMD1 (1705 bp). The constructed phylogenetic tree was based on the maximum likelihood method. It is a commonly used method to reconstruct and represent the evolutionary relationships among the studied organisms, highlighting their evolutionary history and relatedness. This method utilizes a mathematical model of sequence evolution to define the probability that a phylogeny can produce the observed sequences. It then searches for the phylogeny that maximizes this probability (Ranwez, 2002). The Tamura 3-parameter (T92) nucleotide substitution model was identified as the most suitable for constructing the maximum likelihood tree (ML). This determination was based on the scores of the Bayesian Information Criterion (BIC) (Nei and Kumar, 2000). Node support was evaluated with 200 bootstrap replicates. All analyses were conducted in MEGA11 (Tamura et al., 2021).

2.4.Growth assessment: Temperature, irradiance, and nutrients (N/P)

Growth experiments were carried out in batch culture with single strains of *P. reticulatum*. Each experiment was carried out in triplicate. As it is a slow-growing dinoflagellate (Guerrini et al.,

2007; Röder et al., 2012), the growth experiments were performed in a sterilized 50 mL culture bottle containing 20 mL of medium.

The first growth experiment was conducted using three different temperatures15, 20, and 25 °C in an L1 medium with a low irradiance of 20 µmol. m^{-2}. s^{-1}. This low irradiance was chosen to isolate the effect of temperature alone on *P. reticulatum* growth while minimizing the influence of irradiance. This approach allows us to determine the temperature at which the species can effectively use the available light energy for its growth.

The second growth experiment evaluated the effect of increasing irradiance. For this purpose, two additional irradiances, 80 and 130 µmol. m^{-2}. s^{-1}, were tested while maintaining the optimal temperature obtained from the first experiment and using the L1 medium. The different irradiances were measured using a Quantum Apogee Full Spectrum Meter MQ-510.

Finally, the third and final growth experiment evaluated the effect of increasing nitrate and phosphate concentrations. For this, four additional nitrate and phosphate concentrations were tested while maintaining the optimal temperature obtained from the first experiment and the optimal irradiance obtained from the second experiment. The N/P ratio of 24.4, as in the L1 medium of Guillard and Hargraves (1993), was maintained for all other tested concentrations. The tested concentrations were 1.5 × L1, 2 × L1, 2.5 × L1 and 3 × L1, with the L1 medium being 882.4 µM for $NaNO_3$ and 36.2 µM for NaH_2PO_4.

2.5.Estimation of cell abundance

Cell concentration was monitored every two days for most of the time until the beginning of the decline phase. The cultures were gently stirred, and sub-samples of 100 µl were collected under sterile conditions. The culture sub-samples were placed in 5 mL sedimentation tanks supplemented

with sterile seawater and fixed with a Lugol's acid solution. The sedimentation tanks were covered with a glass plate and kept in a dark place. After four hours, cell counts were carried out according to the sedimentation method of Utermöhl (1958) with an inverted microscope. Cell counts were used to calculate the maximum growth rate (μ_m, expressed on divisions day $^{-1}$) during the exponential growth phase using the equation (Guillard, 1973): $\mu = (\text{Ln } N_1 - \text{Ln } N_0)/ t_1 - t_0$. where N_1 and N_0 the cell abundances at the time t_1 and t_0. Time was taken into account from the initiation of the cultures. Average cell density growth curves and average maximum growth rate graphs were generated.

2.6.Toxicity assay

2.6.1. Cell lysis

Cell culture of *P. reticulatum* (30 mL) was harvested at the end of the stationary phase by centrifugation, 30 min at 3500 × g (Pagliara and Caroppo, 2012). The supernatant was removed, and the resulting pellet was resuspended in 2 mL of filtered and sterilized seawater and homogenized. To ensure cell disruption, the sample was processed in three freeze-thaw cycles (one cycle is 24 h) and centrifuged at 1500 × g for 5 min at room temperature after each cycle (Mejía-Camacho et al., 2021). The cell suspension was sonicated with an ultrasound probe (Branson ultrasonic corporation) thrice for 10 min on ice. The sonicated sample was checked under the microscope to ensure cell lysis. The sample was left on ice for 1 h in the dark before centrifugation at 20,000 × g for 30 min. The lysate supernatant was recovered and stored at -80 °C until use (Pagliara and Caroppo, 2012).

2.6.2. Acute toxicity assay

The dried cysts of the brine shrimp *Artemia salina* (brand: Ocean Nutrition, ref: 154085) were hatched in sterile seawater (1 g cysts in 1L of seawater) at 25 °C under constant light and aeration. After 24 h of incubation, *A. salina* nauplii (one day) were collected.

For this purpose, *P. reticulatum* was grown under the optimal growth conditions identified at the end of our growth experiments, as described in section 3.2 of the results of this study. The culture was harvested during the late stationary phase, as described in previous studies conducted by Röder et al. (2012), Sala-Pérez et al. (2016), Liu et al. (2017), and Wang et al. (2019), who also harvested their cultures in this specific growth phase.

An acute toxicity test with cell lysate was performed to examine the effects of intracellular metabolites (Mejía-Camacho et al., 2021). The cell lysate was diluted successively using a dilution factor of 2. The concentrations obtained were 5.30×10^5, 2.65×10^5, 1.33×10^5, 0.66×10^5, and 0.33×10^5 cells. mL^{-1}. Then, ten *A. salina* nauplii were exposed to 100 µL of each cell lysate concentration. Filtered and sterilized seawater was used as the negative control. The test was conducted in 96-well microplates, incubated at 25 °C in the dark (Pagliara and Caroppo, 2012). For each concentration, three replicates were performed. After 24 hours, nauplii that showed no movement of the appendages during ten seconds of observation were considered dead, and the results are expressed as the percentage of dead nauplii after 24 hours (Laza-Martinez et al., 2011). For the *A. salina* bioassay, the lethality rate ± standard error of the mean (SEM) was calculated for each concentration. $SEM=SD/\sqrt{n}$, with SD: standard deviation and n: sample size. The LC_{50} value was determined using probit analysis as Finney (1971) described with Microsoft Excel version 2013 software.

2.7. LC-MS/MS analysis of YTX group

P. reticulatum was grown under the optimal growth conditions stated in section 3.2 of the results of this study in a 1L Erlenmeyer flask containing 500 mL of culture medium. Cell density was determined using the Utermöhl sedimentation method (1958) by sampling 1 mL aliquots once a week, taking into account the volume of the culture and the slow growth of the specie observed in our previous experiments. When the culture reached the early decline stationary phase at 26 days, it was divided into three homogeneous fractions of 150 mL each. The cell concentration of each fraction was determined using the sedimentation method of Utermöhl (1958). Subsequently, each culture fraction was collected and filtered using a 47 mm diameter GF/F microfilter. For sample preparation, 4 mL of methanol was added to the filters, and then the content was homogenized and subjected to an ultrasonic ice bath for 5 min. Three successive extractions were performed with 100 % methanol, LC/MS grade (Brand WWR Chemicals). After centrifugation at 4300 × g for 2 min at 4 °C, the obtained supernatants were pooled, evaporated to dryness under nitrogen flow, and finally recovered in 1 mL of 100 % methanol LC/MS grade (Brand WWR Chemicals).

Sample analyses (two aliquots per each sample) were performed on a UFLC (model UFLC, Shimadzu) coupled to a triple quadrupole mass spectrometer (4000 Qtrap, ABSciex) equipped with a turboV® ESI source. Chromatographic separation was carried out on a C18 Kinetex column (100 Å, 2.6 µm, 100 × 2.1 mm, Phenomenex) with a C18 guard column (4 × 2.0 mm, 2.6 µm, Phenomenex). A binary mobile phase was used, phase A (100 % aqueous) and phase B (95 % aqueous acetonitrile), both containing 2 mM ammonium formate and 50 mM formic acid. The flow rate was 0.4 mL. min^{-1} and the injection volume was 5 µL. The column and sample temperatures were 40 °C and 4 °C, respectively. A gradient elution was used, starting with 20 % B, rising to 95

% B over 6 min, held for 3 min, then decreased to 20 % B in 0.5 min and held for 3 min to equilibrate the system. Negative acquisition experiments were established using the following source settings: curtain gas set at 25 psi at – 4500 V, ion spray at a temperature of 6000 °C, gas 1 and 2 sets, respectively, at 40 and 60 psi, and an entrance potential of -13 V. These parameters had been previously optimized using toxin standards. The mass spectrometer was operated in multiple reaction monitoring (MRM), analyzing the two product ions per compound; for each of the toxins in the YTX group (YTX, homo-YTX, 45-OH-YTX, 45-OH-homo-YTX, COOH-YTX, homo-COOH-YTX), the first transition, the most intense, is used for quantification (Table 1). Certified YTX and homo-YTX calibration solutions were obtained from the National Research Council of Canada (NRCC, Halifax, NS, Canada). The detection limits were 1.7 pg. cell^{-1} and 1.3 pg. cell^{-1} for YTX and homo-YTX, respectively, and the quantification limits were 5.0 pg. cell^{-1} and 3.8 pg. cell^{-1} for YTX and homo-YTX, respectively.

2.8.Statistical Analysis

Statistical comparisons were conducted to evaluate the effects of the different experimental conditions tested (temperature, irradiance, nutrients) on the maximum cell density and growth rate of *P. reticulatum* and the lethal effect of the *P. reticulatum* cell lysate. These comparisons were carried out using a one-way analysis of variance (ANOVA) with a significance level of α=0.05, followed by Tukey's HSD post-hoc test. In cases where the homogeneity of variances and normality of data were not confirmed, non-parametric tests were employed, such as the Kruskal-Wallis test and the Mann-Whitney post-hoc test. All statistical tests were performed with SPSS v. 22.0 statistic software for Windows (IBM).

3. Results

3.1. Morphological and molecular identification

The P. reticulatum cells obtained in cultures are oval to polygonal thecal species with a hypotheca larger than the epitheca and slightly longer than wide (Fig.1). Vegetative cells contained many golden-brown chloroplasts (Fig.1A). The cingulum was located above the median line and was deeply incised (Fig.1B). The surface of the theca had reticulated ornamentation (Fig.1C). The mean cell length was 31.33 ± 5.17 µm (range 25.13- 43.60 µm), and the mean widt+h was 24.19 ± 2.95 µm (range 20.28-32.97 µm).

Molecular analysis of the 18S rDNA gene, which generated a sequence of 1705 nucleotides, confirmed the identity of our strain of *P. reticulatum* isolated from the Atlantic coast of Morocco. The alignment of the sequence of our study species with the results obtained under Blast using GenBank (NCBI) was identical to the other sequences of *P. reticulatum* strains. Our examined strain, *P. reticulatum* IMD1, exhibited a 100 % identical SSU rDNA sequence to other *P. reticulatum* strains (AY421790, AB727656, AB727655, AB727654, and MK995623) from South Korea, Canada, Sweden, Japan, and unidentified location, except for strains AF274273 and DQ217789, which showed a slight genetic difference from the other strains of *P. reticulatum*, as indicated in the maximum likelihood tree (Fig. 2). Furthermore, it was evident from the tree that our strain belonged to the monophyletic clade of *P. reticulatum*.

3.2.Optimization of the growth parameters of *Protoceratium reticulatum*

The growth curves of *P. reticulatum* cultures exposed to three temperatures (15, 20, and 25 °C) under an irradiance of 20 µmol. m^{-2}. s^{-1} in L1 medium are shown in Fig. 3A. The growth was strongly affected by temperature; the highest cell density was found at 20 °C (2000 cells. mL^{-1}),

with a maximum growth rate of 0.24 div. day^{-1} and cell death at 15 and 25 °C under irradiance of 20 µmol. m^{-2}. s^{-1} (Fig. 4A).

Cultures exposed to 80 and 130 µmol. m^{-2}. s^{-1} at 20 °C and L1 medium were the earliest to reach their highest cell density (i.e., at day 23 and 21, respectively), while the slowest was the culture at 20 µmol. m^{-2}. s^{-1} (i.e., at day 37). However, the highest cell density was found at 20 µmol. m^{-2}. s^{-1} (2000 cells. mL^{-1}), followed by those at 80 µmol. m^{-2}. s^{-1} (1237 cells. mL^{-1}) and 130 µmol. m^{-2}. s^{-1} (987 cells. mL^{-1}) (Fig. 3B). Statistical analyses revealed significant differences (ANOVA, Tukey's HSD test, $p < 0.05$) between the maximum cell density obtained at 20 µmol. m^{-2}. s^{-1} and those obtained at irradiance levels of 80 and 130 µmol. m^{-2}. s^{-1}. The maximum growth rate of *P. reticulatum* under these three irradiances ranged from 0.24 to 0.29 div. day^{-1} (Fig. 4B).

The irradiance of 80 µmol. m^{-2}. s^{-1} resulted in the highest maximum growth rate, reaching 0.29 div. day^{-1}, closely followed by the irradiance of 130 µmol. m^{-2}. s^{-1}, which displayed a maximum growth rate of 0.27 div. day^{-1}. Finally, irradiance of 20 µmol. m^{-2}. s^{-1} exhibited the lowest maximum growth rate, with only 0.24 div. day^{-1}. Despite the increase in growth rate at the highest irradiances (80 and 130 µmol. m^{-2}. s^{-1}), no significantly different effect was observed on the maximum growth rate of *P. reticulatum* with the irradiance of 20 µmol. m^{-2}. s^{-1} (ANOVA, $p > 0.05$). Thus, for the rest of the experiment, the irradiance of 80 µmol. m^{-2}. s^{-1} was chosen.

The growth curves of *P. reticulatum* cultures exposed to five different concentrations of medium at 20 °C under 80 µmol. m^{-2}. s^{-1} are shown in Fig. 3C. The medium 3 × L1 produced the highest maximum cell density (6923 cells. mL^{-1}), followed by 2 × L1 (4503 cells. mL^{-1}), 1.5 × L1 (3037 cells. mL^{-1}), 2.5 × L1 (2297 cells. mL^{-1}) and finally L1 produced the lowest cell density (1237 cells. mL^{-1}). The ANOVA test and Tukey's HSD post hoc test ($p < 0.05$) indicate a significant difference between certain maximum cell concentrations (Table 2). Specifically, the maximum cell density

obtained with the 3 × L1 medium was significantly higher than those obtained with the other concentrations of the medium tested. The maximum growth rate of *P. reticulatum* cultures exposed to five different medium concentrations are shown in Fig. 4c. It ranged from 0.24 to 0.29 div. day^{-1}. The L1 and 3 × L1 medium showed the same maximum growth rate among all the medium, with a value of 0.29 div. day^{-1}. The 1.5 × L1 medium exhibited a slightly lower maximum growth rate of 0.28 div. day^{-1}. The 2 × L1 and 2.5 × L1 medium showed the lowest maximum growth rates, with values of 0.26 div. day^{-1} and 0.24 div. day^{-1}, respectively (Fig. 4C). However, there was no significant difference in the maximum growth rate of *P. reticulatum* for the five nutrient concentrations tested (ANOVA, $p > 0.05$).

Therefore, considering the maximum growth rates results, we conducted the toxicity experiments by maintaining our cultures at 20 °C and irradiance of 80 µmol. m^{-2}. s^{-1} and using the L1 culture medium. These conditions were chosen as optimal for the growth of our *P. reticulatum* strain.

3.3. *Artemia salina* acute bioassay

The percentage of lethality in *A. salina* induced by the concentrations of *P. reticulatum* cell lysate is shown in Table 3. Only the concentrations that induced the lethality are reported. The *P. reticulatum* cell lysate was lethal from 0.66 × 10^5 cells. mL^{-1} with 3.3 % lethality. The highest concentration of cell lysate tested (5.30 × 10^5 cells. mL^{-1}) gave 53.3 % lethality in *A. salina*. The calculated LC_{50} value obtained after 24 h was 5.20 × 10^5 cells. mL^{-1}.

The Kruskal-Wallis test ($p = 0.05$) and Mann-Whitney post hoc test ($p < 0.05$) demonstrated that the highest tested cellular lysate concentration (5.30 × 10^5 cells. mL^{-1}) resulted in significantly different lethality in *A. salina* compared to the other concentrations.

3.4. Toxin profile

Among the toxins of the YTX group searched (YTX, homo-YTX, 45-OH-YTX, 45-OH-homo-YTX, COOH-YTX, homo-COOH-YTX) in triplicate culture extracts of *P. reticulatum*, the LC-MS/MS analysis revealed only the presence of YTX at an average concentration of 27.0 ± 2.60 pg YTX cell^{-1}. Figure 5 shows the specific qualitative (1141.4 > 855.6) and quantitative (1141.4 > 1061.6) MRM transitions for YTX in both the standard solution and the *P. reticulatum*, allowing formal identification of YTX.

4. Discussion

4.1. Morphological and molecular identification

Protoceratium reticulatum is described by Lassus et al. (2016), cells oval in shape, sometimes becoming somewhat polygonal. Cingulum is displaced by approximately its width and located anterior to the middle of the cell, making the hypotheca larger than the epitheca. Sulcus was not reaching the antapex. The vegetative cells contain numerous brown chloroplasts, and the cell surface is highly reticulated, making it difficult to evaluate the plate pattern. This morphological description corresponds to our strain of *P. reticulatum* isolated from the coasts of Agadir and agrees with that of several other authors (Table 4). The morphological identification of our strain was confirmed by molecular analysis. In the present maximum likelihood tree (Fig. 2) of the small subunit (SSU) 18S rDNA, the sequence of the clonal strain isolated in this study matches the same clade as the *P. reticulatum* cysts isolated from Saroma Lake, Hokkaido, Japan (AB727654), the Swedish Kattegat coast (AB727655) Brentwood Bay, British Columbia, Canada (AB727656) (Mertens et al., 2012) and the Adriatic Sea in Italy (DQ217789). In the study by Mertens et al. (2018), the sequences obtained after gene analysis of the variable regions of the small subunit show that *Pentaplacodinium saltonense* and *Protoceratium reticulatum* form two distinct clades. This is

also the case in this study. Furthermore, in the study by Liu et al. (2017), the molecular analysis of the 18s rDNA of *P. reticulatum* strains isolated from Japan and the USA belonged to the same *P. reticulatum* clade as the strain in our study. However, by ITS sequence analysis, the *P. reticulatum* strains of Liu et al. (2017) belonged to a geographically widely distributed clade, which includes coasts of the Atlantic, Mediterranean, Pacific, and Arctic waters. Therefore, our *P. reticulatum* strain could also belong to this clade; however, an analysis of the ITS region of our strain would be needed to confirm this.

4.2. Growth experiment

The growth rate is a significant parameter in the dynamics and ecology of the phytoplankton population, as it integrates many biochemical and environmental factors. Among these factors, temperature is important; indeed, it significantly influences phytoplankton dynamics and geographical distribution (Guerrini et al., 2007). In our study, we observed that the temperature associated with low irradiance (20 µmol. m^{-2}. s^{-1}) severely affected the growth of the *P. reticulatum* strain from the Atlantic coast of Agadir. We found that the strain only showed cellular growth at 20 °C, with a maximum growth rate of 0.24 div. day^{-1}, while progressive cell mortality was observed at 15 °C and 25 °C. These results suggest that under low irradiance conditions, 20 °C is the optimal temperature that promotes the photosynthesis process and the growth of our *P. reticulatum* strain. However, the observed cell mortality at 15 °C may be due to its association with a low irradiance of 20 µmol. m^{-2}. s^{-1}. Indeed, low temperatures lead to a reduction in nutrient consumption, photosynthesis efficiency, and growth rates (Claquin et al., 2008; Pittera et al., 2014). However, it is also possible that the species' growth can be affected when combined with low irradiance, as in our study. Studies conducted by Lim et al. (2006) on the growth assessment of two species of *Alexandrium* in discontinuous clonal cultures revealed that the growth rates of these two

species increased with increasing temperature and irradiance. However, the two species showed no net growth under the combination of a low irradiance of 10 µmol. m^{-2}. s^{-1} and a low temperature of 15 °C, although the cells remained alive, unlike in our case. According to Morales (2014), the growth rate increases with temperature below the optimum, but only when the limitation does not come from a lack of light or nutrients. Furthermore, Paz et al. (2006) considered an irradiance of 25 µmol. m^{-2}. s^{-1} to be very low and prevent proper development of *P. reticulatum* cultures. They also defined the common temperature range for species growth in marine environments as between 15 and 23 °C. Furthermore, contrary to this present study, *P. reticulatum* in the northwest Adriatic Sea in Italy, the North Sea in Germany, and the Arctic in Greenland exhibited the highest growth or the best growth rate at temperatures ranging from 15 °C to 16 °C under irradiance ranging from 30 to 120 µmol. m^{-2}. s^{-1} (Guerrini et al., 2007; Röder et al., 2012; Sala-Pérez et al., 2016). These irradiances were higher than the one to which we subjected our cultures. These studies further support the idea that the mortality observed in *P. reticulatum* strain cultures at 15 °C may be associated with its low irradiance of 20 µmol. m^{-2}. s^{-1}.

However, observed cell mortality at 25 °C cannot be attributed to this association, as other studies conducted by Guerrini et al. (2007), Röder et al. (2012) and Sala-Pérez et al. (2016) are also consistent with our results. Despite high irradiance levels, these studies have shown that *P. reticulatum* growth was affected or nonexistent at 25 °C and above.

The results obtained for the different levels of irradiance tested show that cultures subjected to higher irradiance levels (80 and 130 µmol. m^{-2}. s^{-1}) at a temperature of 20 °C and cultured in the L1 medium reached their maximum cell density more rapidly. However, the maximum cell density for cultures exposed to lower irradiance (20 µmol. m^{-2}. s^{-1}) was significantly higher. Furthermore, although higher irradiances promoted an increase in growth rate, no significant effect was

observed. Regarding the growth rate, our results suggest that irradiances range from 20 to 130 µmol. m^{-2}. s^{-1} similarly promotes the growth of our *P. reticulatum* strain. In contrast, several studies on microalgae growth assessment report that increasing irradiance increases maximum cell density and maximum growth rate (Paz et al., 2006; Lim et al., 2006; Meseck et al., 2005). For example, Paz et al. (2006) studied the combined effect of irradiance, temperature, and salinity on the growth of *P. reticulatum* isolated from Spain. Their study revealed that irradiance was the main independent variable in almost all combinations. It positively affected all dependent variables, such as maximum cell density, maximum growth rate, and toxin production. They also found that the positive effect on growth occurred within an irradiance range of 50 to 90 µmol. m^{-2}. s^{-1}. Other studies, such as Erga et al. (2015), on *P. reticulatum* isolated from Norway, observed positive phototaxis and a maximum growth rate ranging from 0 to 0.27 div. day^{-1} for irradiances ranging from 25 to 400 µmol. m^{-2}. s^{-1}. However, Seamer (2001) found that the best growth occurred at an irradiance of 45 µmol. m^{-2}. s^{-1}.

On the other hand, the decrease in maximum cell density obtained at higher irradiances (80 and 130 µmol. m^{-2}. s^{-1}) can have two possible hypotheses. Firstly, this decrease may be due to an adaptation of *P. reticulatum* to these irradiances, reducing the photosynthesis rate. Indeed, as light intensity increases, photosynthesis becomes less efficient, which can decrease growth rate and biomass production, especially under stressful conditions such as very high or low irradiances (Minhas et al., 2016; Wijffels et al., 2010). Furthermore, high irradiance levels can lead to light saturation, exposing the organisms to more light energy than they can effectively utilize in photosynthesis. To cope with this, organisms may employ protective mechanisms such as dissipating excess energy as heat, distributing light energy among different photosynthetic

complexes, or synthesizing photoprotective compounds at the expense of their growth (Bonente et al., 2012; Perelson, 2002; Bernard and Remond, 2012).

The other hypothesis is that the decrease in maximum cell density may be attributable to increased nutrient consumption (nitrate and/or phosphate), creating a limiting factor for the growth of *P. reticulatum* and, thus, a decrease in biomass. Indeed, studies have reported that nitrogen and phosphate can potentially limit (Bergström et al., 2008) and co-limit (Zohary et al., 2005) the growth of phytoplankton in natural aquatic environments as well as in monoculture cultures (Pahlow et al., 2009; Bougaran et al., 2010). Furthermore, a study by Gonçalves et al. (2016) on the effects of irradiance and temperature on growth and nutrient uptake by certain microalgae showed that increased irradiance and temperature resulted in more efficient nutrient consumption by species.

However, as we could not evaluate nitrate and phosphate at the end of the experiments, this hypothesis was not tested in our present study and cannot be excluded as a possible explanation. Nonetheless, the second hypothesis appears to be more plausible since the results of our study demonstrated an increase in the maximum cell density of *P. reticulatum* when the concentrations of nitrate and phosphate in the culture medium were increased under an irradiance of 80 µmol. m^{-2}. s^{-1}, thus supporting this second hypothesis.

The experience of simultaneously increasing the concentration of nutrients (nitrate and phosphate) in the culture medium for the growth assessment of *P. reticulatum* revealed that the most concentrated medium, 3 × L1, led to a significantly higher maximum cell density compared to the other cultures medium, resulting in a cell density six times higher than that of the L1 medium. Although the L1 medium is commonly used for dinoflagellate culture (Guillard and Hargraves, 1993), it is inadequate to maintain a high biomass concentration (Rodríguez et al., 2007; Rodríguez

et al., 2009). In their studies, they observed that to maximize growth rate and biomass yield, it is necessary to provide higher amounts of nutrients, particularly nitrate and phosphate, compared to those present in natural blooms. However, in our study, increasing nutrient concentration had no significant effect on maximum growth rates ranging from 0.24 to 0.29 div. day^{-1}.

Rodríguez et al. (2009), who examined the effect of independent increases in nitrate and phosphate concentrations in *P. reticulatum* cultures medium, concluded that variations in nitrate concentrations did not affect the growth rate and cell density of the specie, while phosphate had an effect up to six times higher. Furthermore, Guerrini et al. (2007) demonstrated that severe phosphate deficiency significantly inhibited the growth of *P. reticulatum*. On the other hand, nitrate limitation and slight phosphate limitation resulted in statistically similar growth compared to the conventional L1 medium. These two studies highlight that an increase in phosphate leads to an increase in the growth rate of *P. reticulatum*. However, in our study, we did not evaluate which of these two nutrients, nitrate or phosphate, was absorbed in the end of the experiments, nor the effect of independent increases in each nutrient on the cell density and growth rate of the species. However, several authors agree that the L1 medium provides sufficient nitrogen for microalgae growth (Leong and Taguchi, 2004; Shi et al., 2005; Rodríguez et al., 2009).

4.3. Toxicity

Marine algal toxins affect the early life stages of vertebrate and invertebrate species (Vasconcelos et al., 2010). Therefore, understanding the potential ecological impact of these algal toxins requires an assessment of their effects on these marine organisms. In the case of the yessotoxins group, very few studies are available on their effects on marine organisms. In this study, the brine shrimp test was used. The intracellular metabolites produced by *P. reticulatum* had a statistically significant impact on the survival of *A. salina* (table 3). Therefore, the lethal effect of *P. reticulatum* lysate

observed on *A. salina* nauplii could be due to YTX. Indeed, LC-MS/MS analysis showed that the *P. reticulatum* strain isolated from the Atlantic coast of Agadir, cultivated under a temperature of 20 °C, irradiance of 80 µmol. m^{-2}. s^{-1}, and in L1 culture medium, could produce yessotoxin at an average concentration of 27.0 ± 2.6 pg YTX $cell^{-1}$. Several studies agree that yessotoxin is the main toxin produced by *P. reticulatum* (Eiki et al., 2005; Paz et al., 2007; Sala-Pérez et al., 2016; Wang et al., 2019).

Furthermore, several factors have been reported to influence the production of YTXs in cultures, such as temperature, salinity, light, growth phase, and nutritional conditions (Seamer, 2001; Paz et al., 2006; Guerrini et al., 2007; Röder et al., 2012). These studies, conducted on algae from different geographical regions, have yielded conflicting results in some cases. For instance, Seamer (2001) found that a strain from New Zealand optimally produced YTX at a light intensity of 45 µmol. m^{-2}. s^{-1}, while Paz et al. (2006), working on a strain from Spain, observed positive YTX production within a range of 50 to 90 µmol. m^{-2}. s^{-1}. Röder et al. (2012) found a higher concentration of YTX in a German strain at a temperature of 15 °C, whereas Guerrini et al. (2007) in Italy observed a higher content at 26 °C.

Despite the complex relationship between *P. reticulatum* and the accumulation of YTXs in shellfish due to varying toxin levels within cells among distant populations of the same species or even within isolates from a single population (Álvarez et al., 2011; Paz et al., 2013; Sala-Pérez et al., 2016), yessotoxins have caused shellfish contaminations in numerous coastal sites. Shellfish contaminations have been reported on the Caucasian coast of the Black Sea in the Russian Federation (Morton et al., 2007), the west coast of the United States (Howard et al., 2008), the northern Yellow Sea in China (Liu et al., 2017), the northwest Adriatic Sea in Italy (Rubini et al., 2021), etc.

The absence of reports on the adverse effects of YTXs on humans prompted the European Commission to increase the health threshold in 2013 from 1 to 3.75 mg YTX equivalent kg^{-1} shellfish meat (European Community, 2013). However, in Morocco, although no bloom of *P. reticulatum* has been reported so far, a "phytoplankton early warning system" for *P. reticulatum* (with a threshold set at 10^3 cells. L^{-1}) in coastal waters has already been established by the National Institute of Fisheries Research (https://www.inrh.ma/inrh). This system aims to improve the monitoring of shellfish farming areas for contamination by yessotoxins and enable optimal prevention in the event of potential blooms of this species along the Moroccan coastline.

5. Conclusion

This study represents the first approach to characterizing toxic and/or harmful dinoflagellate species along the Moroccan Atlantic coasts. The studied species of *P. reticulatum* showed optimal growth at a temperature of 20 °C and low irradiance (20 µmol. m^{-2}. s^{-1}). The increase in irradiance and nutrient concentrations tested did not significantly affect the maximum growth rate of the species. However, the lower irradiance of 20 µmol. m^{-2}. s^{-1} resulted in a significantly higher cell density than 80 and 130 µmol. m^{-2}. s^{-1} irradiances. This suggests that these higher irradiances potentially stimulated increased nutrient consumption, leading to a limiting factor for the species' growth. This hypothesis is supported by the observation that the most concentrated medium in nitrate and phosphate, 3 × L1, resulted in a significantly higher and different maximum cell density than the other tested concentrations. LC-MS/MS analysis revealed that our strain cultivated at a temperature of 20 °C, irradiance of 80 µmol. m^{-2}. s^{-1}, and in L1 culture medium produced YTX at an average concentration of 27.0 ± 2 .6 pg YTX $cell^{-1}$, which could be responsible for the observed lethal effect in *Artemia salina*. However, additional studies are planned to understand better the optimal conditions that influence the proliferation of *P. reticulatum* in the Moroccan Atlantic.

These studies will aim to examine the simultaneous and combined interaction of factors such as temperature, irradiance, nutrient concentration, and other parameters that influence the growth of this dinoflagellate. Studies on the variation and independent increase of nutrients in cultures and their quantification at the end of the experiments will be conducted to understand this strain's nutritional requirements better. Furthermore, studies on the quantification of *P. reticulatum* toxicity under different culture conditions will be conducted to assess potential adverse effects of its blooms on the marine ecosystem. Thus, our present study and these additional studies will contribute to a better understanding of the factors influencing the growth of this species and enable the implementation of appropriate management measures to preserve the marine ecosystem, particularly shellfish, and consequently protect consumer health.

CRediT authorship contribution statement

Moussavou-Mouity Cyrielle Amour: Conceptualization, Formal analysis, Validation, Visualization, Writing - Original draft, Writing - Review & Editing. **Bennouna Asmae**: Conceptualization, Validation, Writing - Review & Editing, Visualization. **Ababou Bouchra**: Writing - Review & Editing, Validation, Visualization. **Amzil Zouher:** Methodology, Validation, Writing - Review & Editing. **Fabienne Herve:** Methodology, Validation, Writing - Review & Editing. **Simon Tanniou:** Methodology, Validation.

6. Acknowledgments

This work was supported by the National Institute of Fisheries Research of the Agadir region (INRH). Thanks to Hassan First University and the Faculty of Science and Technology of Settat which allowed this collaboration. The authors thank the General Director of INRH, Mr. Abdelmalek FARAJ, the Director of the Regional Center of INRH Agadir, Mr. Salaheddine EL

AYOUBI, and the responsible for the laboratory for monitoring the quality of the marine environment (LSSMM) Mr. Rachid ABOUABDELLAH for their material support during the study. The authors also thank Mrs. Amina BOUHALAOUI, who kindly provided us with *Artemia salina*, Mr. EL HAYANE, and Mr. ARAABAB for their technical support during the study.

7. Conflict of interest

The authors declare no conflict of interest.

8. Bibliography

Akselman, R., Krock, B., Alpermann, T.J., Tillmann, U., Borel, M., Almandoz, G.O., Ferrario, M.E., 2015. *Protoceratium reticulatum* (Dinophyceae) in the austral Southwestern Atlantic and the first report on YTX-production in shelf waters of Argentina. Harmful Algae. 45, 40-52. https://doi.org/10.1016/j.hal.2015.03.001

Álvarez, G., Uribe, E., Díaz, R., Braun, M., Mariño, C., Blanco, J., 2011. Bloom of the Yessotoxin producing dinoflagellate *Protoceratium reticulatum* (Dinophyceae) in Northern Chile. J. Sea Res. 65, 427–434. https://doi.org/10.1016/j.seares.2011.03.008

Aune, T., Sørby, R., Yasumoto, T., Ramstad, H., Landsverk, T., 2002. Comparison of oral and intraperitoneal toxicity of yessotoxin towards mice. Toxicon. 40(1), 77–82.

Bergström, A., Jonsson, A., Jansson, M., 2008. Phytoplankton responses to nitrogen and phosphorus enrichment in unproductive Swedish lakes along a gradient of atmospheric nitrogen deposition. Aquatic Biology. 4, 55–64. https://doi.org/10.3354/ab00099

Bernard O., Remond B., 2012. Validation of a simple model accounting for light and temperature effect on microalgal growth. Bioresource technology. 123 :520–527.

Bonente, G., Pippa, S., Castellano, S., Bassi, R., Ballottari, M., 2012. Acclimation of *Chlamydomonas reinhardtii* to different growth irradiances. Journal of Biological Chemistry. 287(8), 5833–5847. https://doi.org/10.1074/jbc.m111.304279

Bougaran, G., Bernard, O., Sciandra, A., 2010. Modeling continuous cultures of microalgae colimited by nitrogen and phosphorus. Journal of Theoretical Biology. 265(3), 443–454. https://doi.org/10.1016/j.jtbi.2010.04.018

Ciminiello, P., Dell-Aversano, C., Fattorusso, E., Forino, M., Magno, S., Guerrini, F., Pistocchi, R., Boni, L., 2003. Complex yessotoxins profile in *Protoceratium reticulatum* from northwestern Adriatic Sea revealed by LC-MS analysis. Toxicon. 42, 7–14. https://doi.org/10.1016/s0041-0101(03)00094-1

Claquin, P., Probert, I., Lefebvre, S., Véron, B., 2008. Effects of temperature on photosynthetic parameters and TEP production in eight species of marine microalgae. Aquatic Microbial Ecology. 51, 1‑ 11. https://doi.org/10.3354/ame01187

Draisci, R., Ferretti, E., Palleschi, L., Marchiafava, C., Poletti, R., Milandri, A., Ceredi, A., Pompei, M., 1999. High levels of yessotoxin in mussels and presence of yessotoxin and homoyessotoxin in dinoflagellates of the Adratic Sea. Toxicon. 37, 1187-1193.

Eiki, K., Satake, M., Koike, K., Ogata, T., Mitsuya, T., Oshima, Y., 2005. Confirmation of yessotoxin production by the dinoflagellate *Protoceratium reticulatum* in Mutsu Bay. Fish Sci. 71, 633–638. https://doi.org/10.1111/j.1444-2906.2005.01009.x

Erga, S.R., Olseng, C.D., Aarø, L.H., 2015. Growth and diel vertical migration patterns of the toxic dinoflagellate *Protoceratium reticulatum* in a water column with salinity

stratification: the role of bioconvection and light. Mar Ecol Prog Ser. 539, 47-64. https://doi.org/10.3354/meps11488

European Community, 2013. Commission Regulation (EC) No. 786/2013 of 16 August 2013 amending Annex III to Regulation (EC) No. 853/2004 of the European Parliament and of the Council as regards the permitted limits of yessotoxins in live bivalve molluscs. Official Journal of the European Union. L220:14.

Finney, D. J., 1971. Probit analysis. Cambridge University Press, New York, 333 p.

Franchini, A., Marchesini, E., Poletti, R., Ottaviani, E., 2004. Acute toxic effect of the algal yessotoxin on Purkinje cells from the cerebellum of Swiss CD1 mice. Toxicon. 43, 347–352. https://doi.org/10.1016/j.toxicon.2004.01.013

Gonçalves, A. C., Pires, J. C., Simões, M., 2016. The effects of light and temperature on microalgal growth and nutrient removal: an experimental and mathematical approach. RSC Advances, 6(27), 22896–22907. https://doi.org/10.1039/c5ra26117a

Guerrini, F., Ciminiello, P., Dell'Aversano, C., Tartaglione, L., Fattorusso, E., Boni, L., Pistocchi R., 2007. Influence of temperature, salinity and nutrient limitation on yessotoxin production and release by the dinoflagellate *Protoceratium reticulatum* in batch-cultures, Harmful Algae. 6(5), 707-717. https://doi.org/10.1016/j.hal.2007.02.006

Guillard, R. R. L., 1973. Division rates. In: Handbook of phycological methods: Cultures methods and growth measurements. Stein J. R., (ed), pp. 290–311, Cambridge University Press, Cambridge, UK.

Guillard, R. R. L., Hargraves, P. E., 1993. *Stichochrysis immobilis* is a diatom, not a chrysophyte. Phycologia. 32(3), 234–236.

Hansen, G., Moestrup, Ø., Roberts, K.R., 1997. Light and Electron Microscopical observations on *Protoceratium reticulatum* (Dinophyceae). Arch. Protistenkd. 147, 381-391.

Howard, M.A.D., Silver, M., Kudela, R.M., 2008. Yessotoxin detected in mussel *(Mytilus californicus)* and phytoplankton samples from the U.S. west coast. Harmful Algae. 7(5), 646–652. https://doi.org/10.1016/j.hal.2008.01.003

Lassus, P., Chomérat, N., Hess, P., Nézan, E., 2016. Toxic and Harmful Microalgae of the World Ocean / Micro-algues toxiques et nuisibles de l'océan mondial. Denmark, International Society for the Study of Harmful Algae / Intergovernmental Oceanographic Commission of UNESCO. IOC Manuals and Guides, 68.

Laza-Martinez, A., Orive, E., Miguel, I., 2011. Morphological and genetic characterization of benthic dinoflagellates of the genera *Coolia*, *Ostreopsis* and *Prorocentrum* from the south-eastern Bay of Biscay. European Journal of Phycology. 46(1), 45–65. https://doi.org/10.1080/09670262.2010.550387

Leong, S.C.Y., Taguchi, S., 2004. Response of the dinoflagellate *Alexandrium tamarense* to a range of nitrogen sources and concentrations: growth rate, chemical carbon and nitrogen, and pigments. Hydrobiologia. 515, 215-224. https://doi.org/10.1023/B:HYDR.0000027331.49819.a4

Lim, P. T., Leaw, C. P., Usup, G., Kobiyama, A., Koike, K., Ogata, T., 2006. Effects of light and temperature on growth, nitrate uptake, and toxin production of two tropical dinoflagellates: *Alexandrium tamiyavanichii* and *Alexandrium minutum* (dinophyceae). Journal of Phycology. 42(4), 786–799. https://doi.org/10.1111/j.1529-8817.2006.00249.x

Liu, L., Wei, N., Gou, Y., Li, D., Liang, Y., Xu, D., Liu, R., Sui, S., Jiang, T., 2017. Seasonal variability of *Protoceratium reticulatum* and yessotoxins in Japanese scallop *Patinopecten yessoensis* in northern Yellow Sea of China. Toxicon, 139, 31–40. https://doi.org/10.1016/j.toxicon.2017.09.015

Mejía-Camacho, A.L., Durán-Riveroll, L.M., Cembella, A.D., 2021. Toxicity Bioassay and Cytotoxic Effects of the Benthic Marine Dinoflagellate *Amphidinium operculatum*. Journal of Xenobiotics. 11(2), 33-45.

Mertens, K.N., Bringué, M., Van Nieuwenhove, N., Takano, Y., Pospelova, V., Rochon, A De Vernal, A., Radi, T., Dale, B., Patterson, R.T., Weckström, K., Andrén, E., Louwye, S., Matsuoka, K., 2012. Process length variation of the cyst of the dinoflagellate *Protoceratium reticulatum* in the North Pacific and Baltic-Skagerrak region: calibration as an annual density proxy and first evidence of pseudo-cryptic speciation. Journal of quaternary science, 27(7), 734–744. https://doi.org/10.1002/jqs.2564

Mertens, K.N., Carbonell-Moore, M.C., Pospelova, V., Head, M.J., Highfield, A., Schroeder, D., Gu, H., Andree, K.B., Fernandez, M., Yamaguchi, A., Takano, Y., Matsuoka, K., Nézan, E., Bilien, G., Okolodkov, Y., Koike, K., Hoppenrath, M., Pfaff, M., Pitcher, G., Al-Muftah, A., Rochon, A., Lim, P.T., Leaw, C.P., Lim, Z.F., Ellegaard, M., 2018. *Pentaplacodinium saltonense* gen. et sp. nov. (*Dinophyceae*) and its relationship to the cyst-defined genus *Operculodinium* and yessotoxin-producing *Protoceratium* reticulatum. Harmful Algae, 71, 57–77. https://doi.org/10.1016/j.hal.2017.12.003

Meseck, S. L., Alix, J. H., Wikfors, G. H., 2005. Photoperiod and light intensity effects on growth and utilization of nutrients by the aquaculture feed microalga, *Tetraselmis chui*

(PLY429). Aquaculture. 246 (1–4), 393 404. https://doi.org/10.1016/j.aquaculture.2005.02.034

Miles, C.O., Samdal, I.A., Aasen, J.A.G., Jensen, D.J., Quilliam, M.A., Petersen, D., Briggs, L.M., Wilkins, A.L., Rise, F., Cooney, J.M., MacKenzie, A.L., 2005. Evidence for numerous analogs of yessotoxin in *Protoceratium reticulatum*. Harmful Algae. 4, 1075–1091.

Minhas, A. K., Hodgson, P., Barrow, C. J., Adholeya, A., 2016. A review on the assessment of stress conditions for simultaneous production of microalgal lipids and carotenoids. Frontiers in Microbiology. 7. https://doi.org/10.3389/fmicb.2016.00546

Morales, J. S., 2014. Liens entre la météorologie et l'abondance de phytoplancton dans l'ocean à partir d'images satellites [Essai, Université de Sherbrooke]. https://savoirs.usherbrooke.ca/handle/11143/7340

Morton, S.L., Vershinini, A., Leighfield, T., Smith, L., Quilliam, M., 2007. Identification of yessotoxin in mussels from the Caucasian Black Sea Coast of the Russian Federation. Toxicon. 50, 581–584. https://doi.org/10.1016/j.toxicon.2007.05.004.

Murata, M., Kumakai, M., Soo Lee, J., Yasumoto, T., 1987. Isolation and structure of yessotoxin, a novel polyether compound implicated in diarrhetic shellfish poisoning. Tetrahedron Lett. 28, 5869–5872. https://doi.org/10.1016/S0040-4039(01)81076-5

Nei, M., Kumar, S., 2000. Molecular Evolution and Phylogenetics. Oxford University Press, New York.

Pagliara, P., Caroppo, C., 2012. Toxicity assessment of *Amphidinium carterae*, *Coolia* cfr. *monotis* and *Ostreopsis* cfr. *ovata* (Dinophyta) isolated from the northern Ionian Sea

(Mediterranean Sea). Toxicon: Official journal of the International Society on Toxinology, 60(6), 1203–1214. https://doi.org/10.1016/j.toxicon.2012.08.005

Pahlow, M., Oschlies, A., 2009. Chain model of phytoplankton P, N and light colimitation. Marine Ecology Progress Series. 376, 69–83. https://doi.org/10.3354/meps07748

Paz, B., Blanco, J., Franco, J.M., 2013. Yessotoxins production during the culture of *Protoceratium reticulatum* strains isolated from Galician Rias Baixas (NW Spain). Harmful Algae. 21-22, 13–19. https://doi.org/10.1016/j.hal.2012.11.002

Paz, B., Riobó, P., Fernández, M.L., Fraga, S., Franco, J.M., 2004. Production and release of yessotoxins by the dinoflagellates *Protoceratium reticulatum* and *Lingulodinium polyedrum* in culture. Toxicon. 44, 251–258. https://doi.org/10.1016/j.toxicon.2004.05.021

Paz, B., Riobó, P., Ramilo, I., Franco, J.M., 2007. Yessotoxins profile in strains of *Protoceratium reticulatum* from Spain and USA. Toxicon. 50, 1–17. https://doi.org/10.1016/j.toxicon.2007.02.005

Paz, B., Vázquez, J. A., Riobó, P., Franco, J., 2006. Study of the effect of temperature, irradiance and salinity on growth and yessotoxin production by the dinoflagellate *Protoceratium reticulatum* in culture by using a kinetic and factorial approach. Marine Environmental Research. 62(4), 286–300. https://doi.org/10.1016/j.marenvres.2006.04.066

Perelson A. S., 2002. Modeling viral and immune system dynamics. Nature Reviews Immunology. 2(1) :28–36.

Pittera, J., Humily, F., Thorel, M., Grulois, D., Garczarek, L., Six, C., 2014. Connecting thermal physiology and latitudinal niche partitioning in marine *Synechococcus*. The ISME Journal. 8(6), 1221‑1236. https://doi.org/10.1038/ismej.2013.228

Ranwez, V., 2002. Méthodes efficaces pour reconstruire de grandes phylogénies suivant le principe du maximum de vraisemblance. Phd thesis, Université Montpellier II - Sciences et Techniques du Languedoc. http://tel.archives-ouvertes.fr/tel-00843175.

Rhodes, L., McNabb, P., Briggs, L., Beuzenberg, V., 2004. Waitaria Bay G14: Yessotoxin in Greenshell™ Mussels and in the Dinoflagellate *Gonyaulax* cf. *spinifera*. Cawthron Report. No. 937. 9 pp.

Röder, K., Hantzsche, F. M., Gebühr, C., Miene, C., Helbig, T., Krock, B., Hoppenrath, M., Luckas, B., Gerdts, G., 2012. Effects of salinity, temperature and nutrients on growth, cellular characteristics and yessotoxin production of *Protoceratium reticulatum*. Harmful Algae. 15, 59-70. https://doi.org/10.1016/j.hal.2011.11.006

Rodríguez, J. J., García, M.del C., Camacho, F. G., Mirón, A. S., Belarbi, el H., Grima, E. M., 2007. New culture approaches for yessotoxin production from the dinoflagellate *Protoceratium reticulatum*. Biotechnology progress. 23(2), 339–350. https://doi.org/10.1021/bp060221u

Rodríguez, J.J.G., Mirón, S. A., García, C.M.C., Belarbi, El H., Camacho, F. G., Chisti, Y., Grima, E.M., 2009. Macronutrients requirements of the dinoflagellate *Protoceratium reticulatum*. 8(2), 239–246. https://doi:10.1016/j.hal.2008.06.002

Rubini, S., Albonetti, S., Menotta, S., Cervo, A., Callegari, E., Cangini, M., Dall'Ara, S., Baldini, E., Vertuani, S., Manfredini, S., 2021. New Trends in the Occurrence of Yessotoxins in the Northwestern Adriatic Sea. Toxins. 13(9), 634. https://doi.org/10.3390/toxins13090634

Sala-Pérez, M., Alpermann, T. J., Krock, B., Tillmann, U., 2016. Growth and bioactive secondary metabolites of arctic *Protoceratium reticulatum* (Dinophyceae). Harmful algae. *55*, 85–96. https://doi.org/10.1016/j.hal.2016.02.004

Salgado, P., Figueroa, R.I., Ramilo, I., Bravo, I., 2017. The life history of the toxic marine dinoflagellate *Protoceratium reticulatum* (Gonyaulacales) in culture. Harmful Algae. 68, 67–81. https://doi:10.1016/j.hal.2017.07.008.

Samdal, I.A., Naustvoll, L.J., Olseng, C.D., Briggs, L.R., Miles, C.O., 2004. Use of ELISA to identify *Protoceratium reticulatum* as a source of yessotoxin in Norway. Toxicon. 44, 75–82. https://doi.org/10.1016/j.toxicon.2004.04.010

Satake, M., Ichimura, T., Sekiguchi, K., Yoshimatsu, S., Oshima, Y., 1999. Confirmation of yessotoxin and 45, 46, 47-trinoryessotoxin production by *Protoceratium reticulatum* collected in Japan. Natural Toxins. 7, 147–150. https://doi.org/10.1002/(sici)1522-7189(199907/08)7:4%3C147::aid-nt50%3E3.0.co;2-6

Satake, M., MacKenzie, L., Yasumoto, T., 1998. Identification of *Protoceratium reticulatum* as the biogenetic origin of yessotoxin. Natural Toxins. 5, 164–167. https://doi.org/10.1002/19970504nt7

Seamer, C., 2001. The production of yessotoxin by *Protoceratium reticulatum*. M.Sc. Thesis, Victoria University of Wellington, pp.172.

Shi, Y., Hu, H., Cong, W., 2005. Positive effects of continuous low nitrate levels on growth and photosynthesis of *Alexandrium tamarense* (Gonyaulacales, Dinophyceae). Phycological Research. 53 (1), 43‐48. https://doi.org/10.1111/j.1440-1835.2005.tb00356.x

Stobo, L.A., Lewis, J., Quilliam, M.A., Hardstaff, W.R., Gallacher, S., Webster, L., Smith, E., McKenzie, M. In: Detection of yessotoxin in UK and Canadian isolates of phytoplankton and optimization and validation of LC-MS methods. Bates S, editor. Gulf Fisheries Centre; Moncton, New Brunswick, Canada: 2003. pp. 8–14.

Suzuki, T., Satake, M., Yoshimatsu, S., Oshima, Y., Horie, Y., Koike, K., Iwataki, M., 2007. Yessotoxin analogues in several strains of *Protoceratium reticulatum* in Japan determined by liquid chromatography-hybrid triple quadrupole/linear ion trap mass spectrometry. Journal of Chromatography A.1142, 172 177. https://doi.org/10.1016/j.chroma.2006.12.048

Tamura, K., Stecher, G., Kumar, S., 2021. MEGA 11: Molecular Evolutionary Genetics Analysis Version 11. Molecular Biology and Evolution. https://doi.org/10.1093/molbev/msab120.

Terao, K., Ito, E., Oarada, M., Murata, M., Yasumoto, T., 1990. Histopatological studies on experimental marine toxin poisoning-5. The effects in mice of yessotoxin isolated from *Patinopecten yessoensis* and of a desulfated derivate. Toxicon. 28, 1095–1104. https://doi.org/10.1016/0041-0101(90)90148-z

Tsuchikane, Y., Hamaji, T., Ota, K., Kato., 2018. Establishment of a clonal culture of unicellular conjugating algae. Journal of Visualized Experiments. 137, 1-7.

Utermöhl, H., 1958. Zur Vervollkommung der quantitativen phytoplancton .Methodik. mitt. int. Ver.Theor. Angrevo. Limnol 9: 1-38.

Vasconcelos, V., Azevedo, J., Silva M., Ramos, V., 2010. Effects of marine toxins on the reproduction and early stages development of aquatic organisms. Marine Drugs 8:59–79. https://doi.org/10.3390/md8010059

Wang, N., Mertens, K. N., Krock, B., Luo, Z., Derrien, A., Pospelova, V., Liang, Y., Bilien, G., Smith, K.F., De Schepper, S., Wietkamp, S., Tillmann, U., Gu, H., 2019. Cryptic speciation in *Protoceratium reticulatum* (Dinophyceae): Evidence from morphological, molecular and ecophysiological data. Harmful Algae. (88). https://doi.org/10.1016/j.hal.2019.05.003

Wijffels, R. H., Barbosa, M. A., Eppink, M. H., 2010. Microalgae for the production of bulk chemicals and biofuels. Biofuels, Bioproducts and Biorefining. 4(3), 287–295. https://doi.org/10.1002/bbb.215

Zohary, T., Herut, B., Krom, M. D., Mantoura, R. F. C., Pitta, P., Psarra, S., Rassoulzadegan, F., Stambler, N., Tanaka, T., Thingstad, T. F., Woodward, E. M. S., 2005. P-limited bacteria but N and P co-limited phytoplankton in the Eastern Mediterranean—a microcosm experiment. Deep-sea Research Part Ii-topical Studies in Oceanography. 52(22–23), 3011–3023. https://doi.org/10.1016/j.dsr2.2005.08.011

Table 1: Transitions used for the negative ion mode MRM detection of YTXs.

	MRM transition Q1>Q3 (*m/z*)
YTX	1141.4>1061.6*/855.6
homo-YTX	1155.6>1075.6* /869.4
45-OH-YTX	1157.5>1077.5*/855.5
45-OH-homo-YTX	1171.5>1091.5*/869.4
COOH-YTX	1173.5>1093.5*/855.5
Homo- COOH- YTX	1187.5>1107.5*/869.5

* Quantifier transition

Table 2: Tukey HSD post-hoc test results for cell concentrations of *P. reticulatum* obtained in the different tested medium.

Multiple Comparisons

Dependent Variable: Cell concentrations

Tukey HSD

(I) Medium	(J) Medium	Mean Difference (I-J)	Std. Error	Sig.	95% Confidence Interval	
					Lower Bound	Upper Bound
L1	1.5×L1	-1800.000*	366.072	.004	-3004.77	-595.23
	2×L1	-3266.667*	366.072	.000	-4471.44	-2061.89
	2.5×L1	-1060.000	366.072	.092	-2264.77	144.77
	3×L1	-5686.667*	366.072	.000	-6891.44	-4481.89
1.5×L1	L1	1800.000*	366.072	.004	595.23	3004.77
	2×L1	-1466.667*	366.072	.017	-2671.44	-261.89
	2.5×L1	740.000	366.072	.323	-464.77	1944.77
	3×L1	-3886.667*	366.072	.000	-5091.44	-2681.89
2×L1	L1	3266.667*	366.072	.000	2061.89	4471.44
	1.5×L1	1466.667*	366.072	.017	261.89	2671.44
	2.5×L1	2206.667*	366.072	.001	1001.89	3411.44
	3×L1	-2420.000*	366.072	.000	-3624.77	-1215.23
2.5×L1	L1	1060.000	366.072	.092	-144.77	2264.77
	1.5×L1	-740.000	366.072	.323	-1944.77	464.77
	2×L1	-2206.667*	366.072	.001	-3411.44	-1001.89
	3×L1	-4626.667*	366.072	.000	-5831.44	-3421.89
3×L1	L1	5686.667*	366.072	.000	4481.89	6891.44
	1.5×L1	3886.667*	366.072	.000	2681.89	5091.44
	2×L1	2420.000*	366.072	.000	1215.23	3624.77
	2.5×L1	4626.667*	366.072	.000	3421.89	5831.44

*. The mean difference is significant at the 0.05 level.

Table 3: Brine shrimp (*Artemia salina*) lethality test for cell lysate and cell-free medium of *P. reticulatum.*

P. reticulatum	**Cells. mL^{-1}**	**Number of *Artemia salina* nauplii**	**Number of deaths**	**Mean deaths**	**Mortality (%)**
Cell lysate	5.30×10^5	10	4	5.33 ± 0.67	53.33
		10	6		
		10	6		
	2.65×10^5	10	3	1.67 ± 0.88	16.67
		10	0		
		10	2		
	1.33×10^5	10	1	0.33 ± 0.33	3.33
		10	0		
		10	1		
	0.66×10^5	10	0	0.33 ± 0.33	3.33
		10	1		
		10	0		
	0.18×10^5	10	0	0.33 ± 0.33	3.33
		10	0		
		10	1		
Control (sea water)		10	0	0	0
		10	0		
		10	0		

Table 4: Comparison of the sizes and morphological characteristics of *Protoceratium reticulatum* from the literature and the result of the present study

Species	Length (µm)	Width (µm)	Shape	Location of specie	References
P. reticulatum	34-39	29-31	Subsphaeroidal with the longitudinal axis larger than transverse, without neck and spines; epitheca shorter than hypotheca; cingulum displacement of 1–2 times its width, descending, without overhang; sulcus narrow, excavated.	Austral Southwestern Atlantic	Akselman et al. (2015)
P. reticulatum	31.1±3.4	-	Generally, subspherical and slightly longer than wide, the cingulum was located above the medline and was deeply incised and displaced by about one cingulum width.	Greenland	Sala-Pérez et al. (2016)
P. reticulatum	30.6-40.8	21.4-35.5	Shorter epitheca than hypotheca vegetative cells have two flagella, one transverse and one longitudinal. They also contain numerous golden-brown chloroplasts and an oval or lobed U-shaped nucleus in the hypotheca's dorsal part.	Southern Chile	Salgado et al. (2017)

Table 4 (continued)

P. reticulatum	35.4-27.1	31.3-25.2	Length slightly longer than width. The cells consist of a conical epithecal part and a hemispherical hypothecal part surrounded by a slightly left cingulum on which small and open pores are uniformly distributed.	Northern Yellow Sea of China	Liu et al. (2017)
P. reticulatum	25.4-47.4	20.5-40.7	The cells were generally polyhedral and slightly longer than wide. The thecae had a rounded epitheca and hypotheca. The cingulum was located in the pre-equatorial part of the cell, descending with a displacement of one cingulum width. The plates were more or less reticulated with numerous pores.	Artic	Wang et al. (2019)
P. reticulatum	25.1-43.6	20.3-32.97	Vegetative cells contain many golden-brown chloroplasts. Epicone crescent-shaped or tongue-shaped in ventral view and much smaller than the descending cingulum of the hypocone. The sulcus was not reaching the antapex. Cell surface highly reticulated, without overhanging; sulcus narrow, excavated.	Agadir Atlantic Morocco	This study

Figure 1

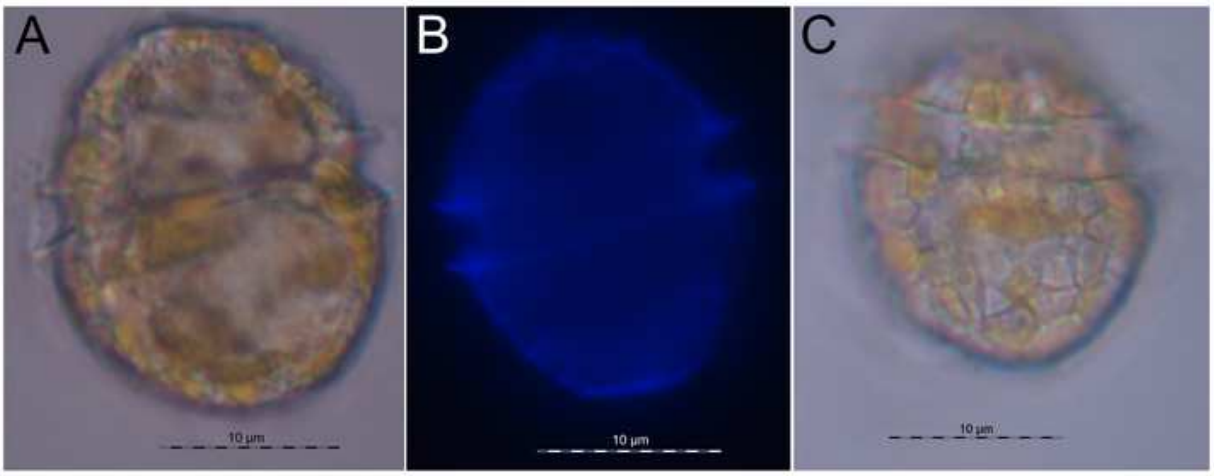

Figure 2

Click here to access/download;Figure;figure 2.tif

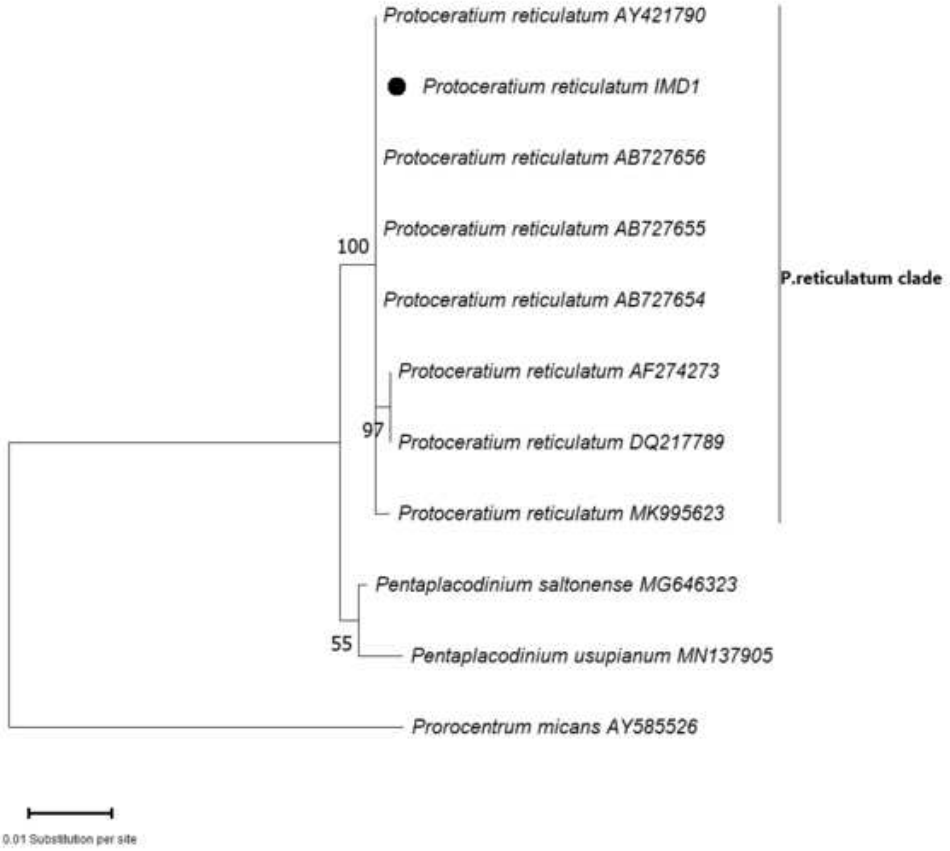

arbre article.tif

Figure 5

Click here to access/download;Figure;figure 5.tif

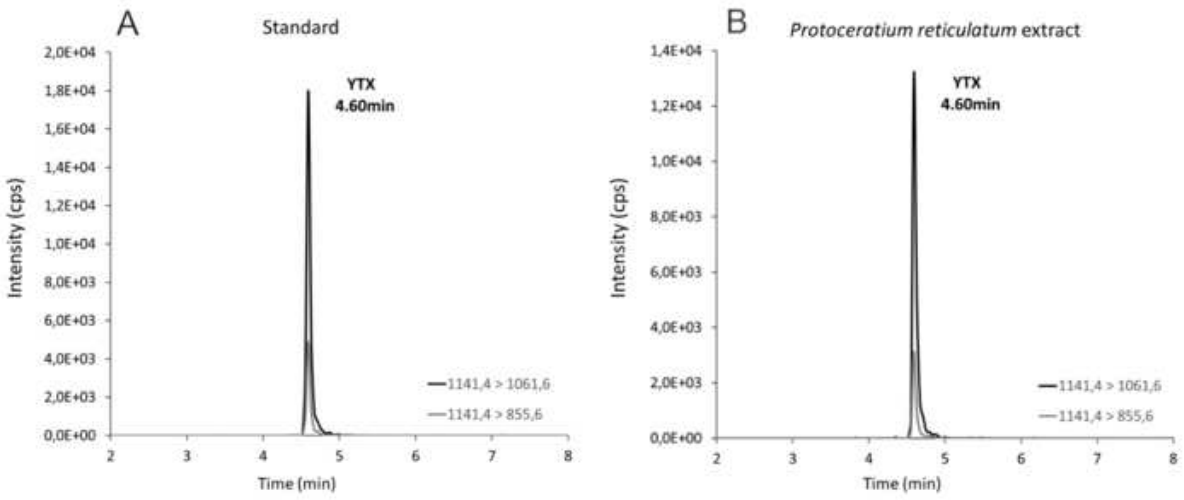

yesso.tif

Figure 3

Click here to access/download;Figure;Figure 03.tif

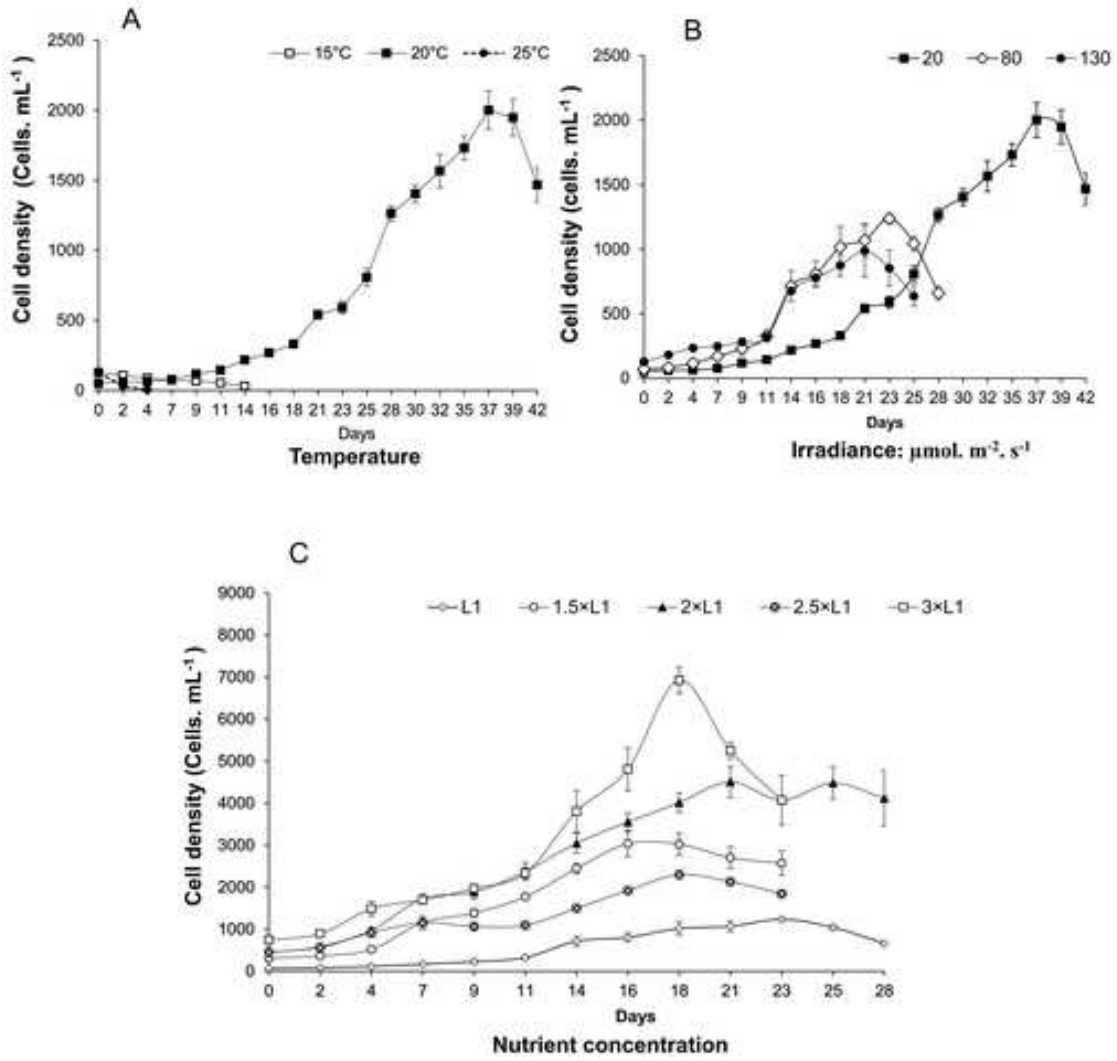

Figure 4

Click here to access/download;Figure;Figure 04.tif

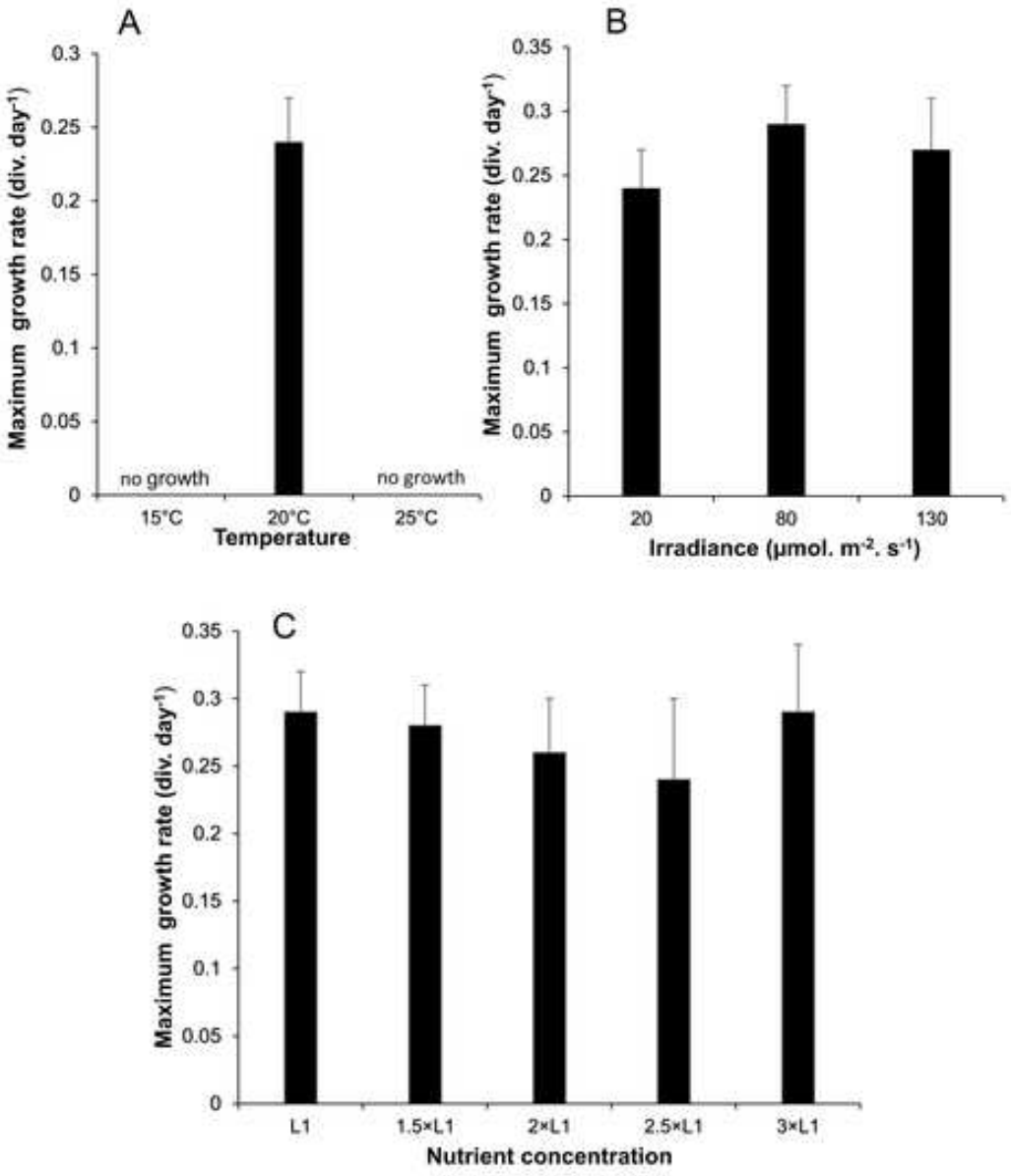

Highlights

- First isolation and culture of the dinoflagellate *P. reticulatum* in Morocco.
- First molecular identification of a *P. reticulatum* strain in Morocco.
- First report about YTX production by *P. reticulatum* isolated in the Atlantic of Morocco.

List of Figures

Figure 1: Micrographs of *Protoceratium reticulatum* cells: light microscopy living vegetative cell with golden-brown chloroplasts (**A)**, fluorescence microscopy of a calcofluor-stained cell showing the shape of the theca and the deeply incised cingulum **(B)** and light microscopy showing the reticulated ornamentation of the cell (**C**).

Figure 2: Phylogenetic tree of *Protoceratium reticulatum* strains based on the 18S rDNA sequence using maximum likelihood (ML). Node support was evaluated with 200 bootstrap replicates. The sequence of the clonal strain in this study is marked with a black circle. Other sequences are identified by taxonomic name and a GenBank accession number. The scale bar indicates the average number of substitutions per site.

Figure 3: Average growth curves of *Protoceratium reticulatum* cells in culture at **(A)** temperatures of 15, 20, and 25 °C in L1 medium at 20 µmol. m^{-2}. s^{-1} **(B)** irradiations of 20, 80 and 130 µmol. m^{-2}. s^{-1} in L1 medium at 20 °C **(C)** different nutrient concentrations in 1; 1.5; 2; 2.5 and 3 × L1 at 20 °C and 80 µmol. m^{-2}. s^{-1}. Error bars indicate the standard error of the mean (n=3).

Figure 4: Maximum growth rate of *Protoceratium reticulatum* at **(A)** temperatures of 15, 20, and 25 °C in L1 medium at 20 µmol. m^{-2}. s^{-1} **(B)** under irradiances of 20, 80, and 130 µmol. m^{-2}. s^{-1} in the medium L1 at 20 °C **(C)** at different nutrient concentrations in 1; 1.5; 2; 2.5 and 3 × L1 at 20 °C under 80 µmol. m^{-2}. s^{-1}. Values represent the mean, and the error bars indicate the standard error of the mean (n=3).

Figure 5: LC-MS/MS analysis results **(A)** Standard and **(B)** *P. reticulatum* culture extract.

REGIONAL STUDIES IN MARINE SCIENCE

AUTHOR DECLARATION

Submission of an article implies that the work described has not been published previously (except in the form of an abstract or as part of a published lecture or academic thesis), that it is not under consideration for publication elsewhere, that its publication is approved by all authors and tacitly or explicitly by the responsible authorities where the work was carried out, and that, if accepted, it will not be published elsewhere in the same form, in English or in any other language, without the written consent of the copyright-holder.

By attaching this Declaration to the submission, the corresponding author certifies that:

- The manuscript represents original and valid work and that neither this manuscript nor one with substantially similar content under the same authorship has been published or is being considered for publication elsewhere.

- Every author has agreed to allow the corresponding author to serve as the primary correspondent with the editorial office, and to review the edited typescript and proof.

- Each author has given final approval of the submitted manuscript and order of authors. Any subsequent change to authorship will be approved by all authors.

- Each author has participated sufficiently in the work to take public responsibility for all the content.

Declaration of interests

☒ The authors declare that they have no known competing financial interests or personal relationships that could have appeared to influence the work reported in this paper.

☐ The authors declare the following financial interests/personal relationships which may be considered as potential competing interests: